OXFORD

molecular human reproduction

Molecular Human Reproduction, 2026, **32(1)**, gaaf062

https://doi.org/10.1093/molehr/gaaf062

Advance Access Publication Date: January 6, 2026

Original Research

Embryo secretome regulation of the endometrial epithelial transcriptome: development of a model to test for embryo viability

Zhixing Jin[1,2,†], Yifan Wang[1,†], Abigail Freeman Blatchford[1], Helena Rodriguez-Caro[1,3], Luyao Wang[1], Christian M. Becker[1], Pedro Melo[1], Tim Child[1], Rebecca Dragovic[1], Ingrid Granne[1], and Jennifer H. Southcombe[1,*]

[1]Nuffield Department of Women's and Reproductive Health, University of Oxford, Oxford, UK
[2]Department of Obstetrics and Gynecology, The First Affiliated Hospital of Soochow University, Suzhou, People's Republic of China
[3]Department of Oncology, University of Lausanne and Ludwig Institute for Cancer Research, Lausanne, Switzerland

*Correspondence address. Nuffield Department of Women's and Reproductive Health, University of Oxford, L3 Women's Centre, JR Hospital, Oxford OX3 9DU, UK. E-mail: jen.southcombe@wrh.ox.ac.uk https://orcid.org/0000-0003-0699-650X

†These authors contributed equally to this work.

ABSTRACT

The aim of this study was to develop an advanced *in vitro* model of human endometrium using single-cell-derived endometrial epithelial organoids, enabling the study of embryo secretome–endometrial crosstalk at the maternal–fetal interface. Single-cell-derived organoids generated from endometrial tissue of a parous 39-year-old woman recapitulated hormone-responsive decidualization, as demonstrated by expression of SPP1 and acetyl-α-tubulin. When cultured in embryo culture media, organoid viability was maintained with no cytotoxicity, but proliferation was suppressed, likely due to the lower concentrations of the required factors in organoid growth media. Organoids were stimulated with culture supernatants from morphologically good-quality embryos with known pregnancy outcomes (live birth (n = 4) vs no pregnancy (n = 4)). Transcriptomic profiling (RNA-sequencing) revealed that 32 genes were differentially expressed (DEGs) in organoids exposed to the culture supernatants from live-birth embryos versus non-pregnant outcomes: 24 upregulated and 8 downregulated. These DEGs were enriched for biological processes related to cell motility and cytoskeletal dynamics. In conclusion, soluble factors secreted by human blastocysts achieving live birth selectively modulate the endometrial epithelial transcriptome, enhancing pathways involved in cytoskeletal remodeling and immune modulation. This embryo-directed remodeling likely facilitates endometrial receptivity for successful implantation to occur. Our organoid model provides a robust platform for further investigating implantation failure.

Keywords: endometrial epithelial organoids / embryo culture supernatant / embryo–endometrial dialogue / *in vitro* model / transcriptome

Introduction

Human embryo implantation occurs in the window of implantation (WOI), in the secretory phase of the menstrual cycle. During this period, the endometrium undergoes physiological modifications providing maximum endometrial receptivity, giving a favorable environment for the implanting embryo (Ashary *et al.*, 2018). Successful embryo implantation requires the processes to synchronize, i.e. a good-quality embryo encounters a fully receptive endometrium, so appropriate crosstalk between the embryo and endometrium can occur (Awonuga *et al.*, 2023). Alterations to these molecular and cellular interactions during the WOI can negatively affect the success of a pregnancy.

The World Health Organization estimates that 10% of couples worldwide will struggle with infertility (Carson and Kallen, 2021). Many will require the use of ARTs, often *in vitro* fertilization and embryo transfer (IVF-ET), to establish pregnancy (Thoma *et al.*, 2013). Despite significant advancements in IVF-ET techniques, embryo implantation failure represents one of the main limiting factors for IVF outcome. Indeed, about one-third of unsuccessful implantations may be ascribed to embryo aneuploidy, which becomes more common as maternal age increases due to associated oocyte abnormalities. The remaining two-thirds are due to altered endometrial receptivity (Mackens *et al.*, 2017).

The two-way dialogue between the maternal endometrium and the embryo during the WOI has been reported to be fundamental for the embryo implantation: in addition to direct cell–cell interactions, the embryo secretes different types of proteins, RNA and DNA, as well as enzymes, metabolites, and extracellular vesicles (Aplin and Ruane, 2017; Mishra *et al.*, 2021). However, in humans, very little is still known about embryo–endometrial interactions, largely due to ethical issues and the difficulty of establishing reliable and reproducible *in vitro* models of human endometrium. The recent development of 3D culture techniques, such as spheroids, organoids, or assembloids derived from patients, has enabled scientists to mimic the endometrium *in vitro* to begin to investigate the crosstalk mechanisms (Li *et al.*,

Received: September 2, 2025. **Revised:** December 5, 2025. **Accepted:** December 22, 2025

2022). Endometrial epithelial organoids (EEOs) are particularly versatile, as they are polarized, hollow, 3D structures that maintain genetic and phenotypic stability over an extended period of time, and are responsive to hormonal changes (Fitzgerald et al., 2019). Importantly, they not only mirror the pathophysiology of endometrial diseases effectively but are also valuable for preclinical drug testing. Additionally, the application of gene editing techniques further enhances their utility (Lou et al., 2022).

The aim of this study is to investigate embryo–endometrial crosstalk at the maternal–fetal interface with the EEOs model, to elucidate whether the embryo secretome can modify the endometrial genome, contributing to successful pregnancy.

Materials and methods

Ethical approval

Written informed consent was obtained from the patient before endometrial biopsy or oocyte collection and protocols were approved by the Oxfordshire Research Ethics Committee C—the Immunology of Subfertility study (ref: 08/H0606/94).

Patient recruitment and embryo culture supernatant collection

Women <40 years of age undergoing single ET during IVF in Oxford Fertility, UK, were recruited to our study. Women with uterine disorders (endometriosis, fibroid, and adenomyosis), ovarian reserve alteration (polycystic ovary syndrome, primary ovarian insufficiency), or genetic abnormalities were excluded.

Embryos were cultured in the COOK sequential culture media system (COOK Medical, Queensland, Australia) at 37°C in 6% CO_2, 5% O_2 in nitrogen. On the morning of Day 5 of culture, a single blastocyst was selected for transfer to each patient in the study. Once the blastocyst was moved to the transfer dish, ~40 µl culture supernatant was removed from within the oil-immersed droplet and stored at −80°C. Embryo culture supernatants were collected from transfer-grade blastocysts as identified by the Gardner & Schoolcraft grading system (Gardner et al., 2000) on Day 5 of embryonic development. Embryo culture supernatants were selected depending on the pregnancy result: (i) blastocysts which resulted in positive pregnancy and delivered a healthy neonate (n = 4) and (ii) blastocysts that did not implant and resulted in negative pregnancy (n = 4). Patient information is displayed in Supplementary Table S1.

Endometrial biopsies

Endometrial biopsies (1.5–3.0 cm in length, ~0.5 cm in diameter) were collected using a Wallach, Endocell Sampler (CooperSurgical, Trumbull, CT, USA) during the secretory phase of the menstrual cycle. For all co-culture experiments, organoids derived from the endometrium of a 39-year-old woman with previous proven fertility (live birth) were used. Immediately after collection, biopsies were placed in a Petri dish on ice. Tissue was initially preserved in HypoThermosol® FRS solution (Sigma-Aldrich, St. Louis, MO, USA; H4416), then overlaid with ice-cold RPMI 1640 medium (Thermo Fisher Scientific, Waltham, MA, USA; 11875093) supplemented with 10% (v/v) heat-inactivated fetal bovine serum (FBS; Sigma-Aldrich; F7524) (hereafter referred to as RPMI/FBS). The tissue was mechanically minced into fragments <1 mm^3 using sterile techniques, then the suspension was centrifuged at 500×*g* for 3 min. After supernatant removal, the pelleted tissue was resuspended in ice-cold CryoStor® cell cryopreservation medium CS-10 (Sigma-Aldrich; C2874). Samples were aliquoted into cryovials and frozen using a Mr Frosty™ controlled-rate freezing container (Thermo Fisher Scientific; 5100-0001) according to the manufacturer's protocol, followed by long-term storage at −80°C.

Establishment of organoids

Frozen endometrial samples were rapidly thawed at 37°C, transferred to a 15 ml conical tube, and diluted with 13 ml of ice-cold RPMI/FBS. After centrifugation (500×*g*, 5 min, 4°C), the supernatant was discarded. The tissue pellet underwent enzymatic digestion in pre-warmed RPMI/FBS containing 1 mg/ml Collagenase V (Sigma-Aldrich; C9263) and 0.1 mg/ml DNAse I (Roche Plc, Basel, Switzerland; 11284932001). Digestion was performed at 37°C on a MACSMix™ (Miltenyi Biotech, Bergisch Gladbach, Germany) tube rotator (16 rpm), with digestion duration adjusted based on tissue fragment size. Progress was monitored every 15 min using an inverted phase-contrast microscope to assess stromal and epithelial cell dissociation.

Digested tissue was centrifuged (500×*g*, 5 min), resuspended in fresh RPMI 1640, and sequentially filtered through 100- and 40-µm cell strainers (BD Biosciences, San Jose, CA, USA; 352340). The 40-µm strainer was backwashed to collect retained endometrial epithelial cells (EECs). The cell suspension was centrifuged (500×*g*, 5 min), and the pellet was resuspended in ice-cold Matrigel® (Corning, NY, USA; 356231) using pre-chilled low-retention pipette tips (Eppendorf, Hamburg, Germany; 022492062). The mixture was immediately returned to ice.

For organoid culture, 25-µl droplets of the Matrigel-cell suspension were plated in the center of a 48-well plate (Corning; 3548) and polymerized at 37°C, 5% CO_2 for 15 min. Subsequently, 250 µl of organoid expansion medium (ExM; modified as detailed) was carefully overlaid. ExM was composed of: 1× Advanced DMEM/F12 (Life Technologies, Carlsbad, CA, USA; 12634010), 1× B27 Supplement minus Vitamin-A (Life Technologies; 12587010), 100 ng/ml Recombinant human Noggin (Peprotech, Rocky Hill, NJ, USA; 120-10c), 10 ng/ml Recombinant human FGF-10 (Peprotech; 100-26), 1× N2 Supplement (Life Technologies; 17502048), 1.25 mM N-Acetyl-cysteine (Sigma; A9165-5G), 100 µg/ml Primocin (Invivogen, San Diego, CA, USA; ant-pm-1), 500 ng/ml Recombinant human Rspondin-1 (Peprotech; 4645-RS-01M/CF), 2 mM Nicotinamide (Sigma; N0636), 50 ng/ml Recombinant human EGF (Peprotech; AF-100-15), 500 nM ALK-4,-5,-7 Inhibitor, A83-01 (Ti) (Tocris, Bristol, UK; 2939), 1× ITS-G (Life Technologies; 41400045), 2 ng/ml bEGF (Peprotech; AF-100-15-100uG), 10 µM SB202190 (Sigma; S7067-5MG), 1× GlutaMax (100X) (Life Technologies; 35050061), 10 µM Y-27632 (Abcam, Cambridge, UK; 688000), and 1 nM β-estradiol (Sigma; E4389).

Organoids were passaged every 7–10 days. Matrigel-embedded organoids were mechanically dissociated, centrifuged (600×*g*, 6 min), and resuspended in 150 µl Advanced DMEM/F12 medium. Mechanical disruption was achieved through 300 pipetting cycles. After repeating centrifugation, the pellet underwent an additional ~80 pipetting cycles. The dissociated organoids were re-embedded in Matrigel (25 µl/well) and cultured with 250 µl ExM as described above.

Organoid generation from single EECs for co-culture

EEOs were generated from single-cell suspensions using established protocols with modifications. Briefly, ExM was removed from the wells and replaced with 250 µl of ice-cold Cell Recovery Solution (Corning; 354253). After 1 h incubation at 4°C, the solution containing organoids was transferred to LoBind tubes (Eppendorf; 0030108442) using Wide-Bore Low Retention Tips (Eppendorf; 022491021), followed by centrifugation at 600×*g* for 6 min at 4°C.

After supernatant removal, the pellet was subjected to enzymatic dissociation using 1 ml TrypLE Express Enzyme (Thermo Fisher; 12605036) with gentle tube inversion. Digestion was monitored microscopically at 5–10 min intervals to prevent over-digestion, terminating when >90% single cells were generated (typically 20–30 min at 37°C with rotational mixing). The cell suspension was filtered through 40 μm cell strainers and washed five times with pre-warmed Advanced DMEM/F12 medium (Gibco/Thermo Fisher; 12634028).

Following final centrifugation (300×*g*, 5 min), viability was assessed using a TC20 Automated Cell Counter (Bio-Rad, Hercules, CA, USA; 1450102) with Trypan Blue exclusion. Cells were resuspended in Matrigel (Corning; 356231) at 500 cells/μl and plated in 384-well plates (Corning; 3544) using pre-chilled tips (20 μl/well). Polymerization was completed after 15 min incubation at 37°C, 5% CO_2 before adding 90 μl ExM.

Decidualization induction

To induce decidualization, organoids derived from single EECs (passage 3) were subjected to two distinct hormonal regimens: (i) continuous exposure to ExM supplemented with 1 nM β-estradiol (Sigma; E4389) for 14 consecutive days; or (ii) initial priming with ExM supplemented with 1 nM β-estradiol for 7 days followed by 7-day stimulation with 50 ng/ml progesterone (Sigma; P8783) in ExM containing 0.5 nM residual β-estradiol. All cultures were maintained under standard conditions (37°C, 5% CO_2) with medium replacement every 24–48 h.

Embryo supernatant–EEO co-culture

On Day 14 post-culture, following established decidualization protocols, the culture medium was replaced with 35 μl of embryo-conditioned supernatant collected from individual embryos. The decidualized organoids were then co-cultured with embryo supernatants for 24 h under standard culture conditions prior to subsequent RNA isolation and transcriptome sequencing analysis.

Immunofluorescence microscopy

EEOs cultured for 7–12 days in 8-well μ-Slide microscopy chambers (ibidi™ GmbH, Gräfelfing, Germany; 80826) underwent whole-mount immunofluorescence staining. After aspirating the expansion medium, organoids embedded in Matrigel® were fixed with 4% paraformaldehyde (PFA) for 30 min at room temperature (RT). Samples were washed twice with PBS and permeabilized in 0.5% Triton X-100/PBS for 30 min at RT, followed by blocking with 5% bovine serum albumin (BSA)/PBS for 2–3 h at RT. Primary antibody incubation was performed overnight at 4°C with rotation. The secondary antibody was then incubated for 2–3 h at RT. Samples were mounted with mounting medium with DAPI (Abcam; ab104139). Z-stack images were acquired using a Leica TCS SP8 confocal laser scanning microscope.

Antibodies used for Immunofluorescence were: pan-cytokeratin conjugated-Alexa Fluor® 488 (Invitrogen/Thermo Fisher; 53-9003-82; dilution 1:100), E-cadherin conjugated-Alexa Fluor® 647 (Biolegend, San Diego, CA, USA; 147308; dilution 1:100), anti-EpCAM (Cell Signaling Technology, Danvers, MA, USA; 29295; dilution 1:800), anti-SPP1 (Abcam; ab214050; dilution 1:100), anti-Acetyl-α-Tubulin (Cell Signaling Technology; 5335; dilution 1:800), anti-mouse Alexa Fluor® 488 (Invitrogen; A28175; dilution 1:1000), and anti-rabbit Alexa Fluor® 594 (Invitrogen; A11012; dilution 1:1000).

Cell viability

EEOs were treated with embryo culture supernatants collected from IVF-derived human embryos at graded concentrations (20%, 50%, 100% v/v) for 24 h at 37°C/5% CO_2; 70% methanol (Sigma-Aldrich; 322415) was included as a cytotoxicity-positive control and basal ExM was used as the negative control. Following treatment, viability was quantified using the LIVE/DEAD Viability/Cytotoxicity Kit (Thermo Fisher, L3224; Calcein AM: 4 μM, EthD-1: 6 μM). Organoids were incubated with staining solution for 3 h under light-protected conditions, then imaged using Leica TCS SP8 confocal laser scanning microscope with excitation/emission settings: 494/517 nm (Calcein, live cells) and 528/617 nm (EthD-1, dead cells). Three technical replicates per condition were analyzed using ImageJ (v1.53) with automated thresholding to calculate viable cell area percentages ([$Calcein^+$ area]/[$Calcein^+$+$EthD\text{-}1^+$ area] ×100).

RNA isolation and sequencing

Total RNA was isolated from samples using the RNAqueous™-Micro Total RNA Isolation Kit (Thermo Fisher Scientific; AM1912) following the manufacturer's protocol. RNA quality was assessed using the Agilent 2100 Bioanalyzer (Agilent Technologies, Santa Clara, CA, USA) (RIN values were >7) and RNA quantity was measured using the Qubit RNA HS Assay Kit (Thermo Fisher Scientific; Q32852). Normalized RNA samples were used to generate cDNA libraries using the SMARTer® Stranded Total RNA-Seq Kit v3 Pico Input Mammalian (Takara Bio, San Jose, CA, USA; 634485) according to the manufacturer's instructions. The prepared cDNA libraries were quality checked by Source Genomics (Nottingham, UK) for concentration and fragment size distribution. Paired-end sequencing (150 bp) was performed on a NovaSeq X Plus platform (Illumina, San Diego, CA, USA) by Source Genomics.

RNA-sequencing data analysis

Raw-sequencing (RNA-seq) reads were quality-controlled and trimmed using Trim Galore with parameters: paired-end mode, Phred33 quality scores, minimum quality score of 30, and minimum read length of 30 bases. FastQC reports were generated simultaneously for quality assessment. The quality-filtered reads were aligned to the human reference genome (Ensembl GRCh37) using STAR aligner (v2.7.3a). Gene annotations were obtained from Ensembl release 75 in GTF format. Feature counts were generated using the featureCounts function from the Subread package (version 2.0.3).

RNA-seq data analysis was performed using R (version 4.4.2). Raw count normalization and differential expression analysis were conducted using DESeq2, with samples classified into positive and negative pregnancy outcome groups. Genes with adjusted *P*-value <0.05 and absolute log2-fold change >1 were considered differentially expressed. Principal component analysis (PCA) was conducted using DESeq2's variance-stabilizing transformation function. Hierarchical clustering was performed on DESeq2-normalized counts of the top 500 most variable genes using correlation distance and complete linkage. Visualizations were generated using packages including ggplot2, ggrepel, and pheatmap.

Functional enrichment analysis of differentially expressed genes was conducted using clusterProfiler with org. Hs.eg.db annotation database, analyzing Gene Ontology terms and KEGG pathways. Multiple testing correction was performed using the Benjamini–Hochberg method (adjusted *P*-value <0.05). Enrichment results were visualized using enrichplot and DOSE packages.

Results

Single-cell-derived organoids provide a robust *in vitro* model for embryo secretome–endometrial interaction studies

Establishing a standardized EEO model is critical for investigating embryo–endometrial crosstalk. To optimize the generation of purified and homogeneous EEOs within a shortened timeframe, we systematically evaluated three distinct isolation protocols (Fig. 1A), with resulting organoids visualized on Days 1–8 of culture (Fig. 1B).

Method 1 (sequential filtration) involved tissue digestion, then sequential filtration through 100 and 40 μm strainers enabled selective retention of epithelial cell aggregates while excluding stromal contaminants. Although this conventional approach minimized stromal cell contamination, the resulting EEOs exhibited significant heterogeneity in size (50–300 μm diameter) due to variable cell aggregation, precluding precise quantification.

Method 2 (single-cell derivation) was a refinement of Method 1, with TrypLE-mediated dissociation of retained aggregates into single epithelial cells (viability >92%), allowing the generation of monodisperse cultures that formed uniform EEOs (100 ± 25 μm diameter) within 8 days. These organoids demonstrated epithelial integrity through sustained expression of pan-cytokeratin and E-cadherin (Fig. 1C), with stromal contamination below detection limits. Crucially, this protocol enabled precise cell counting for standardized seeding.

Method 3 (selective adhesion) involved stromal cell depletion via differential adhesion, yielding epithelial-enriched supernatants. However, residual stromal contamination necessitated extended passaging (≥3 cycles) to achieve acceptable purity, thereby prolonging culture timelines and increasing experimental variability.

Our findings establish that single-cell-derived EEOs (Method 2) overcome the limitations of conventional aggregation-dependent models by combining rapid production timelines with enhanced reproducibility. The ability to generate size-standardized, quantification-ready organoids from defined cell numbers positions this platform as a transformative tool for high-resolution mechanistic studies of endometrial receptivity. Future work will validate the functional competence of these organoids using hormonal response assays.

Single-cell-derived endometrial organoids recapitulate hormone-responsive decidualization

The lack of consensus regarding β-estradiol supplementation in endometrial organoid culture protocols prompted us to establish

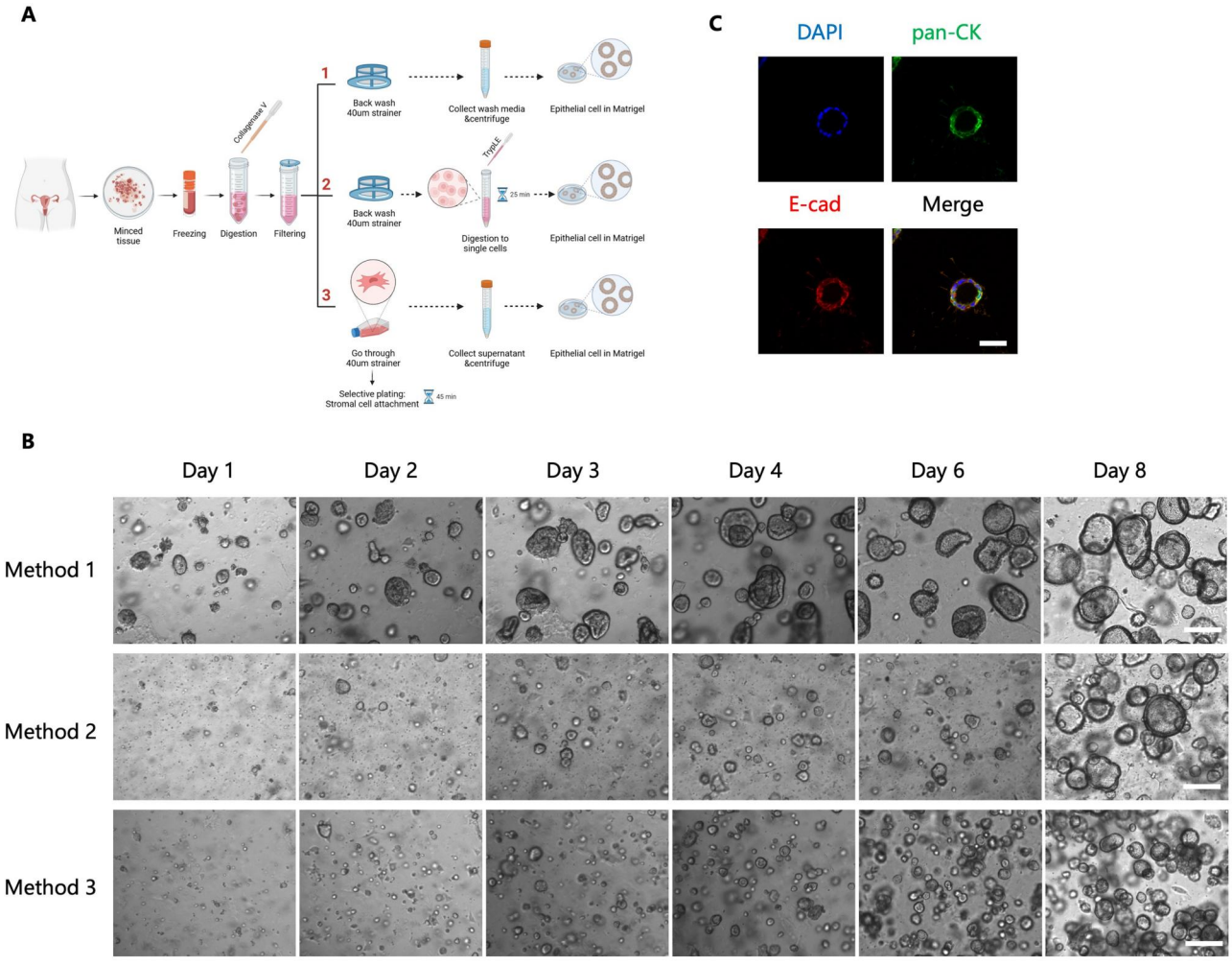

Figure 1. Single-cell-derived organoids provide a robust *in vitro* model for embryo–endometrial interaction studies. (**A**) Schematic diagram displaying three tested methods for EEOs establishment endometrial samples were minced and frozen for future EEO isolation, after thawing samples were digested using collagenase V and filtered prior to proceeding with three alternate methods as described. Image created in BioRender. Wang, Y. (2025) https://BioRender.com/nloh9t0. (**B**) Representative bright-field microscopy images showing the development of EEOs on Days 1–8 using the three different methods. Scale bar, 100 μm. (**C**) Representative confocal microscopy images of EEOs, with antibody labeling of epithelial markers pan-Cytokeratin (CK) (green) and E-cadherin(-cad) (red). Nuclei were stained with DAPI (blue). Scale bar, 50 μm. EEO, endometrial epithelial organoids.

a physiologically relevant cycling model. Building on the previous single-cell RNA-seq findings demonstrating that β-estradiol (E2)-maintained EEOs better preserve native epithelial signatures (Mareckova *et al.*, 2024), we implemented a modified Boretto's protocol (Boretto *et al.*, 2017) to investigate decidualization dynamics (Fig. 2A).

By Day 14, marked morphological divergence emerged between treatment groups. E2-maintained organoids retained spherical morphology with patent lumens, whereas E2+P4 stimulation induced hallmark decidual transformations including darker coloring, thicker luminal walls, and a distorted shape (Fig. 2B). These structural changes correlated with secretory phase biomarker induction. SPP1 and acetylated α-tubulin fluorescence intensity increased significantly in E2+P4 organoids compared to E2-only controls (Fig. 2C and D). Acetylated α-tubulin exhibited apical polarization in progesterone-treated organoids versus E2-maintained cultures. Three-dimensional reconstruction of z-stack images (Videos 1 and 2) revealed spatial coordination between SPP1 accumulation and cytoskeletal remodeling, mirroring *in vivo* secretory phase transformation.

Embryo culture media maintains viability but impairs proliferative capacity of endometrial organoids

While COOK embryo culture medium is clinically established for IVF, its undefined composition raises questions about compatibility with EEO models. Cytotoxicity assessment via dual Calcein AM/EthD-1 (live/dead, respectively) labeling revealed no acute toxicity across concentration gradients (0%, 10%, 20%, 50%, 100%), with >98% viability in all groups after 24-h exposure. Organoids retained structural integrity without morphological alterations, confirming biocompatibility for short-term exposure (Fig. 3A).

To evaluate sustained culturability, we implemented three longitudinal regimens: (i) continuous ExM throughout Days 1–7; (ii) ExM priming (Days 1–3) followed by 100% COOK embryo culture medium (Days 4–7); and (iii) COOK embryo culture medium from initial seeding (Days 1–7).

ExM-maintained organoids exhibited characteristic proliferation, whereas organoids in COOK embryo culture medium showed growth arrest within 48 h, manifesting as size reduction and lumen collapse (Fig. 3B and C). Despite sustained viability (>95% Calcein+ cells) through to Day 7, cells stopped proliferating, confirming the inability of COOK embryo culture medium to support EEO self-renewal (Fig. 3C).

No cytotoxicity was observed across embryo culture supernatant concentrations

We further validated embryo-conditioned supernatant (containing embryonic paracrine factors) for co-culture compatibility. No cytotoxicity was observed across supernatant concentrations (0%, 20%, 50%, 100%), with viability consistently >97% and preserved organoid architecture after 24-h exposure (Fig. 3D),

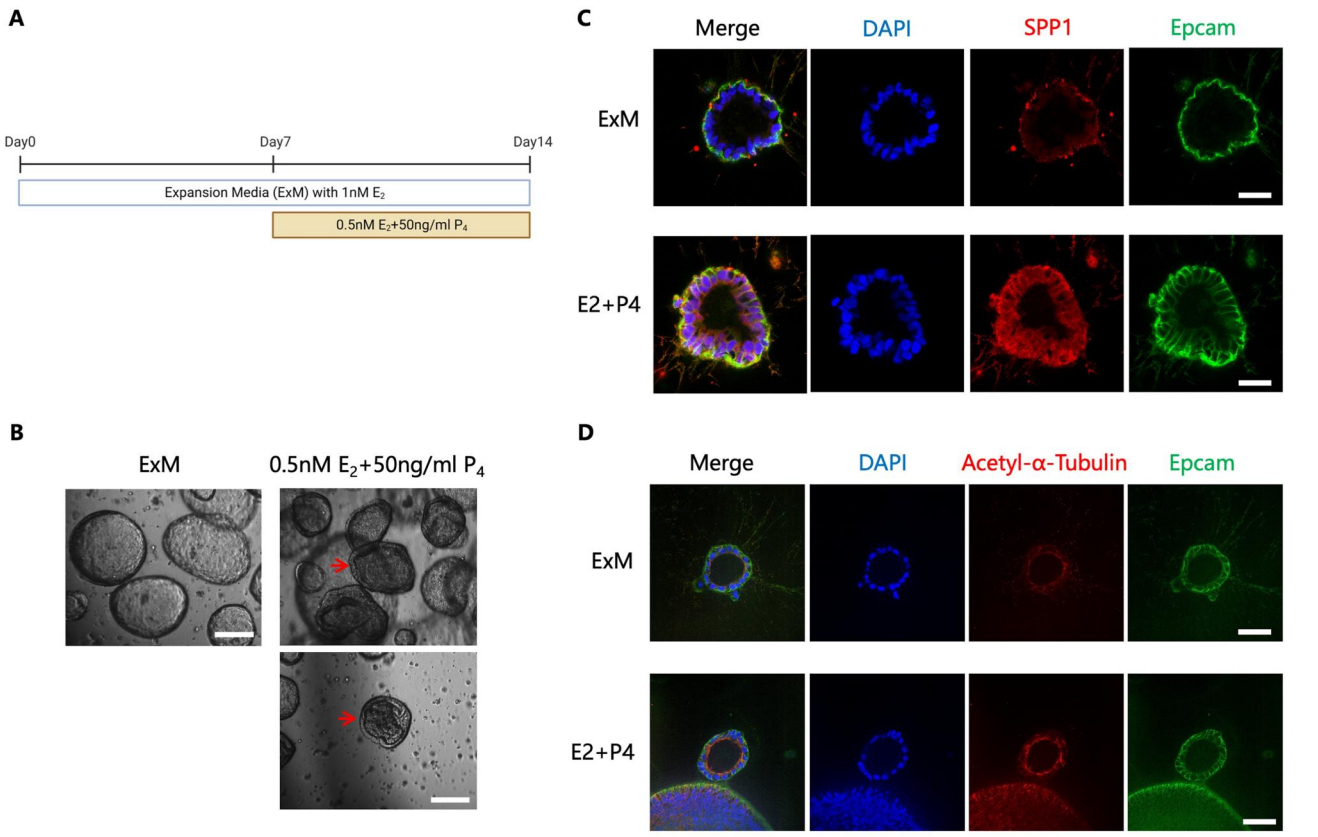

Figure 2. Single-cell-derived endometrial organoids recapitulate hormone-responsive decidualization. (**A**) Schematic diagram showing hormone treatment conditions to induce EEO decidualization. (**B**) Representative bright-field microscopy images showing the development of EEOs at Day 14 after hormone treatment, ExM/1 nM E2 versus 0.5 nM E2 + 50 ng/ml P4. Red arrows indicate an example of tortuous EEOs. Scale bar, 100 μm. Representative confocal microscopy images of EEOs treated with ExM/1 nM E2 versus 0.5 nM E2 + 50 ng/ml P4 for 14 days, and stained with antibodies for epithelial marker EpCAM (green) and decidualized cell marker SPP1 (**C**) or ciliated EEC (cEEC) marker acetyl-α-tubulin (**D**) (red), and nuclei labeled with DAPI (blue). Scale bar, 50 μm. EEO, endometrial epithelial organoids; EEC, endometrial epithelial cells; E2, β-estradiol; P4, progesterone; EpCAM, epithelial cell adhesion molecule; SPP1, secreted phosphoprotein 1.

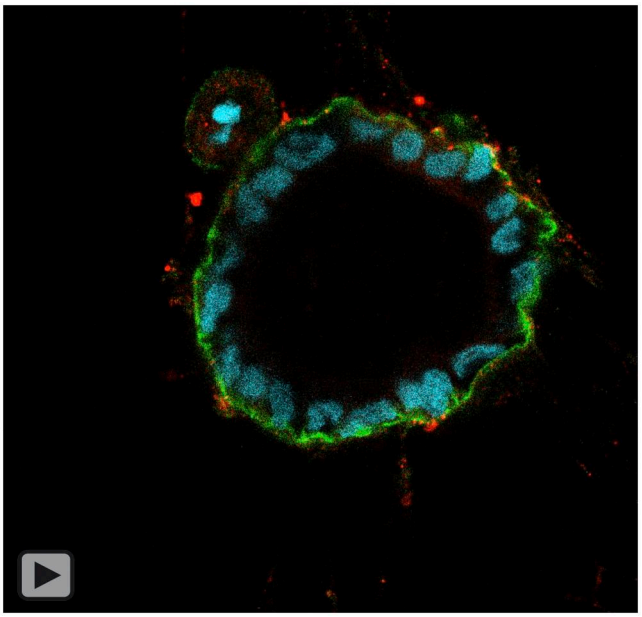

Video 1. First 3D reconstruction of z-stack images of control EEO using confocal microscopy. EpCAM, green; SPP1, red; DAPI nuclear staining, blue. 3D, three-dimensional; EEO, endometrial epithelial organoids.

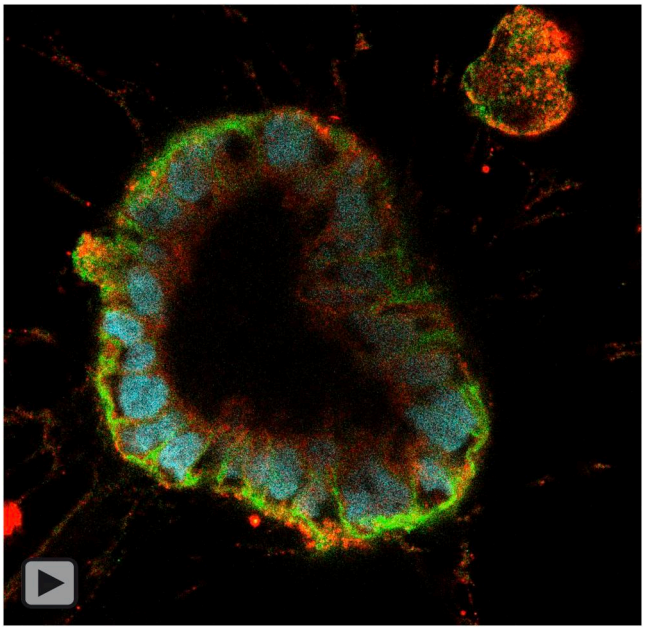

Video 2. Second 3D reconstruction of z-stack images of control EEO using confocal microscopy. EpCAM, green; SPP1, red; DAPI nuclear staining, blue. 3D, three-dimensional; EEO, endometrial epithelial organoids.

indicating its suitability for the following embryo secretome–endometrial interaction studies.

Transcriptomic analysis of EEOs after embryo culture supernatant treatment with known pregnancy outcomes

Hormone-stimulated receptive EEOs were treated with embryo supernatants isolated from morphologically good-quality grade embryos, from eight individuals. The transcriptomic profiles of the positive and negative outcome groups were analyzed using PCA and hierarchical clustering to explore global patterns in gene expression. PCA revealed a distinct separation between the two groups, with the first principal component (PC1) accounting for 50% of the variance and the second principal component (PC2) explaining 33% (Fig. 4A). The positive outcome samples were separated from the negative outcome sample clustering along PC1, indicating significant transcriptomic differences between the groups.

Hierarchical clustering further validated the distinct grouping observed in PCA. Clustering analysis was performed on the top 500 most variable genes, and the resulting heatmap segregated the samples into two clusters corresponding to the positive and negative outcomes (Fig. 4B). This clustering aligns with the trends observed in PCA and highlights the robustness of the transcriptional differences.

A total of 32 genes were identified as differentially expressed between the positive and negative outcome groups, with 24 genes upregulated and 8 genes downregulated in the positive outcome group (Fig. 4C). Differential expression was determined based on an adjusted *P*-value threshold of <0.05 and an absolute log2-fold change >1. To visualize the differential expression data, a volcano plot (Fig. 4D) was generated.

Among the upregulated genes, *VWA5B1* (log2-fold change: 3.01, adjusted *P*-value: 0.007), *FAM157B* (log2-fold change: 2.43, adjusted *P*-value: 0.036), and *ELAPOR1* (log2-fold change: 1.79, adjusted *P*-value: 0.043) demonstrated the highest levels of upregulation. Conversely, the most downregulated genes included *NPM1P24* (log2-fold change: −6.86, adjusted *P*-value: 0.041), *DERL3* (log2-fold change: −2.73, adjusted *P*-value: 0.048), and *HPGD* (log2-fold change: −1.92, adjusted *P*-value: 0.037).

Functional enrichment analysis of the differentially expressed genes provided insights into the biological pathways influenced by embryo-secreted factors (Fig. 4D and E). Gene Ontology (GO) analysis highlighted enrichment in biological processes directly related to cell motility and cytoskeletal dynamics, such as 'microtubule bundle formation' (GO:0001578, adjusted *P*-value: 0.000035) and 'cilium assembly' (GO:0060271, adjusted *P*-value: 0.001069).

Pathway analysis using KEGG revealed significant involvement of the 'Wnt signaling pathway' (hsa04310, adjusted *P*-value: 0.082221), which is known to regulate cytoskeletal reorganization and cellular migration (Fig. 4F). The upregulation of genes involved in the Wnt pathway, including *CFAP157* and *CROCC2*, suggests a role for this pathway in enhancing the motility and adhesion properties of EECs in response to embryo-secreted factors. Additionally, pathways related to immune modulation, such as 'Neutrophil extracellular trap formation' (hsa04613, adjusted *P*-value: 0.082221), may further support the establishment of a receptive endometrial environment.

Discussion

This study elucidates the molecular dialogue between human blastocysts and EEOs, revealing that embryo-secreted soluble factors from successful pregnancies distinctly reshape the endometrial transcriptional landscape. This effect likely occurs in a localized manner at the site where the blastocyst apposes and attaches to the endometrial epithelial lining, as has been indicated by mouse studies (Das *et al.*, 1994). In support of our results, previous data suggested that embryos influence endometrial receptivity (Cuman *et al.*, 2013; Parks *et al.*, 2018). However, these studies used implantation versus no implantation without

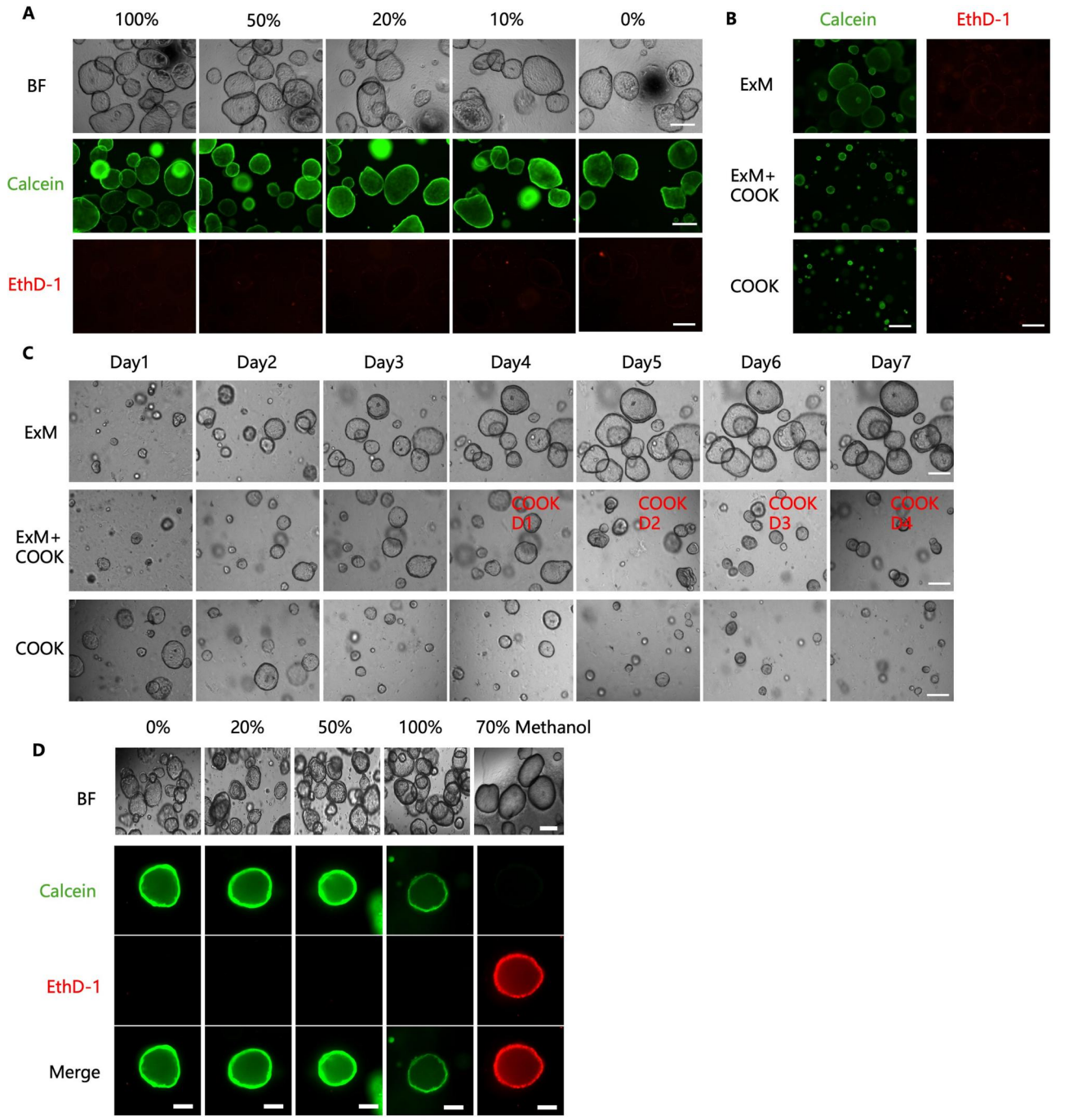

Figure 3. Cytotoxicity assessment of COOK embryo culture media and embryo culture supernatant on endometrial organoids via co-incubation. (**A**) Cytotoxicity assessment via dual Calcein AM (green)/EthD-1 (red) labeling (LIVE/DEAD Viability kit, Thermo Fisher) revealed no acute toxicity across concentration gradients (0%, 10%, 20%, 50%, 100% COOK media), with >98% viability in all groups after 24-h exposure. Scale bar, 100 μm. BF: Bright-field. (**B**) Cytotoxicity assessment via dual Calcein/EthD-1 labeling at Day 7 after COOK embryo culture media or ExM treatment. Scale bar, 100 μm. (**C**) Representative bright-field microscopy images showing the development of EEOs at Days 1–7 treated with COOK embryo culture media or ExM. Scale bar, 100 μm. (**D**) Representative bright-field (BF) microscopy or confocal microscopy images of EEOs stained with dual Calcein AM/EthD-1 labeling for cytotoxicity assessment showing the organoid architecture after 24-h exposure to different concentrations of embryo culture supernatant (0%, 20%, 50%, 100%) or 70% methanol as the cytotoxicity-positive control. Scale bar, 100 μm. EEO, endometrial epithelial organoids; EthD-1, ethidium-1.

consideration of live birth outcome or embryo grade. They also utilized primary epithelial cells cultured in a monolayer, but these lack essential features like complete polarity, have a short lifespan and often become unresponsive to hormonal signals, and are therefore not a viable cellular model system.

The emergence of organoid technologies using human cells has enabled a revolution in modeling the endometrium *in vitro*. Our single-cell-derived organoid protocol minimizes stromal contamination, ensuring reproducibility and uniformity, representing a critical advancement over prior methods. Importantly, the hormone-dependent induction of both architectural and molecular decidual markers (SPP1 and acetyl-α-tubulin), coupled with quantitative validation of morphological parameters, confirms single-cell-derived EEOs cyclic functionality. This system's ability

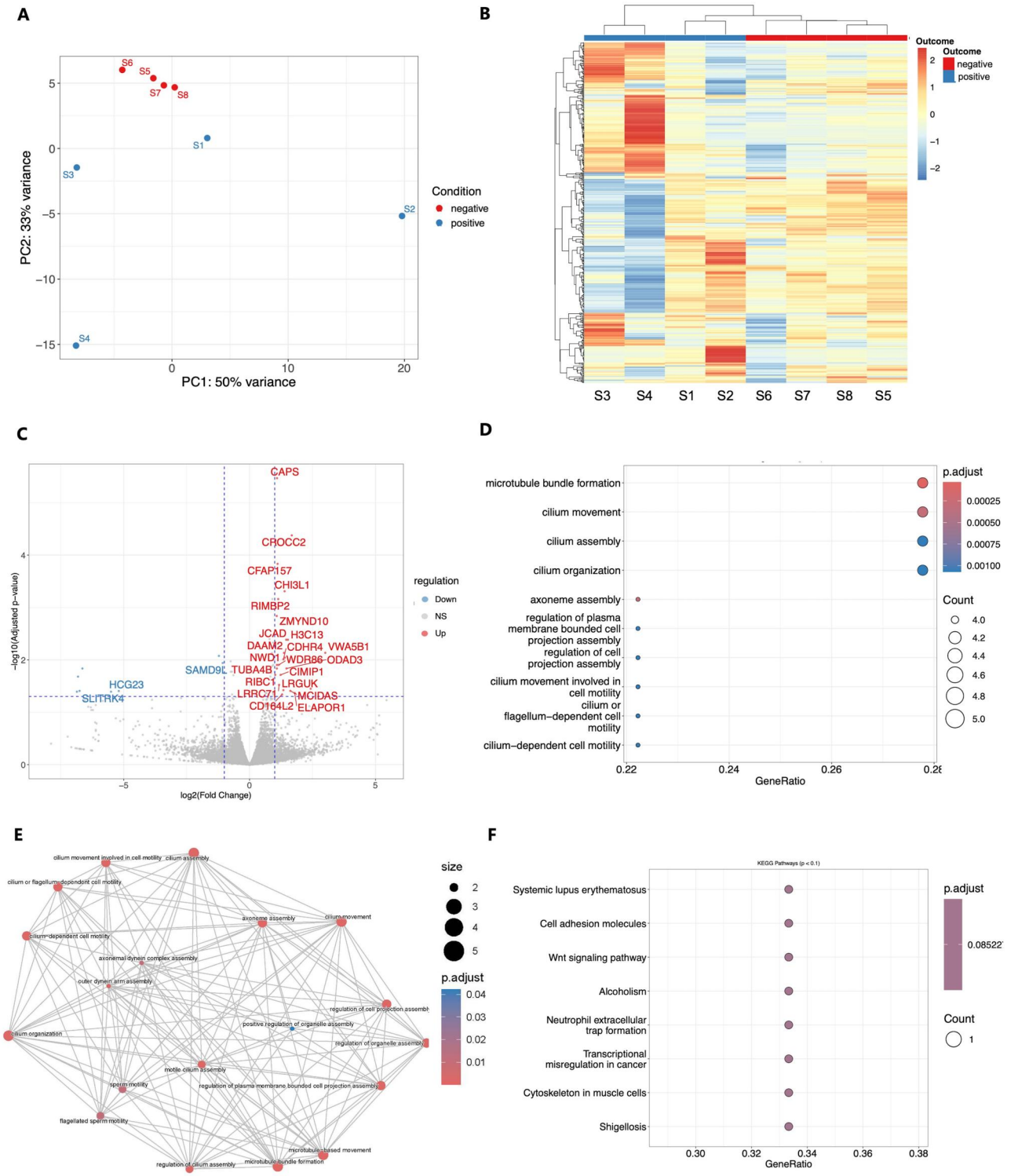

Figure 4. Endometrial epithelial organoids (EEO) RNA transcriptomic changes after embryo culture supernatant co-culture. Decidualized EEO were treated for 24 h with individual embryo culture supernatants from eight embryos resulting in negative pregnancy (n = 4) or live birth (n = 4). Total RNA was extracted and cDNA libraries generated (SMARTer Stranded Total RNA-Seq kit) (Takara Bio) and paired-end sequencing performed (NovaSeq X Plus; Source Genomics) for transcriptomic data analysis. (**A**) PCA plot with distinct separation between the two groups (negative pregnancy vs live birth). (**B**) Heatmap of top 500 variable genes with hierarchical clustering of differentially expressed genes between the samples S1–8, determined by DESeq2. (**C**) Volcano plot of the differentially expressed genes between the groups, highlighting significant genes. (**D, E**) The top 10 significant GO results and enrichment map between the groups. (**F**) The top eight significant pathways identified via KEGG pathway enrichment analyses.

to synchronize structural plasticity with biomarker expression dynamics positions it as a robust platform for investigating embryo–endometrial crosstalk pathways.

After cytotoxicity assessment, embryo culture supernatants from morphologically good-quality embryos for single ET from patients with positive (live birth) or negative pregnancy outcomes

were co-cultured on single-cell-derived organoids. This captured the molecular dialogue between a blastocyst and the endometrium. We optimized culture methodology to generate organoids in 20 μl Matrigel domes formed in a 384-well plate, to permit co-culture with single embryo supernatants (35 μl maximum volume). Our findings demonstrate that soluble factors secreted by human blastocysts with successful implantation and live birth outcomes distinctly modulate endometrial epithelial gene expression, primarily enhancing pathways critical for cytoskeletal remodeling and immune modulation. These are likely to be important in facilitating endometrial receptivity for successful implantation. Importantly, the epithelium independently senses the factors, as there are no stromal/immune cells in this model. These results underscore the embryo's active role in priming endometrial epithelium receptivity.

The upregulation of genes such as *VWA5B1* and *ELAPOR1* in the positive pregnancy group aligns with their known roles in extracellular matrix organization and cell adhesion (Huang *et al.*, 2023). *VWA5B1* encodes von Willebrand factor A domain-containing protein implicated in cell–matrix interactions, potentially facilitating trophoblast anchoring during implantation. *ELAPOR1*, also known as *KIAA1324* or estrogen-induced gene 121 (*EIG121*), encodes a transmembrane protein that functions in lysosomal degradation, autophagy, secretory granule differentiation, and acrosome formation (Cho *et al.*, 2022). In pancreatic β cells, ELAPOR1 inhibits insulin hormone and insulin-like growth factor 1 signaling by decreasing the number of cell-surface receptors and blunting the response to insulin (Siehler *et al.*, 2024). In human tumors, ELAPOR1 is associated with a favorable prognosis in colorectal (Huang *et al.*, 2023), pancreatic (Ohara *et al.*, 2024), endometrial (Meng *et al.*, 2024), and ovarian (Rodriguez *et al.*, 2021) cancers. Similarly, the enrichment of microtubule-related GO terms ('microtubule bundle formation', 'cilium assembly') and activation of the Wnt signaling pathway suggest that embryo-derived factors promote cytoskeletal reorganization in EECs. This is consistent with previous studies where Wnt/β-catenin signaling drives uterine receptivity by regulating EEC polarization and secretory activity (Tepekoy *et al.*, 2015).

The downregulation of *DERL3* and *HPGD* in the positive outcome group further highlights the embryo's ability to suppress inflammatory and immune tolerance. DERL3, is a member of the Derlin family residing in the endoplasmic reticulum. The presence of unfolded or misfolded proteins in the endoplasmic reticulum leads to the upregulation of DERL3, which facilitates the degradation of misfolded glycoprotein (Ye *et al.*, 2004; Oda *et al.*, 2006). Given the association between endoplasmic reticulum stress and inflammation, recent studies have shown that DERL3 can promote the inflammatory response in inflammatory diseases, such as rheumatoid arthritis (Geng *et al.*, 2020) and Crohn's disease (da Silva *et al.*, 2020). In human malignancies, such as colorectal cancer, gastric cancer, and breast cancer, DERL3 has been found to generate a Warburg effect and has tumor suppressor-like properties (Lopez-Serra *et al.*, 2014). In lung adenocarcinoma, DERL3 might serve as an oncogenic molecule in immune suppressive tumor microenvironments by inducing the endoplasmic reticulum-associated degradation process (Lin *et al.*, 2022). *HPGD* encodes 15-hydroxyprostaglandin dehydrogenase (15-PGDH), which is a member of the short-chain non-metallic enzyme alcohol dehydrogenase protein family. This enzyme is primarily responsible for the metabolism of prostaglandins (Sun *et al.*, 2021), which are known to play important roles in a various physiological and cellular processes, such as inflammation. HPGD is downregulated in rheumatoid arthritis synovial tissue, and antirheumatic drugs increase the expression of HPGD in RA fibroblast-like synoviocytes (Kim *et al.*, 2015). Therefore, reduced HPGD expression may prolong prostaglandin signaling, creating a pro-implantation microenvironment.

Furthermore, the differential gene expression profiles between positive and negative pregnancy groups highlight potential biomarkers (e.g. *CFAP157, CROCC2*) for non-invasive assessment of endometrial receptivity. The biocompatibility of embryo-conditioned supernatants supports their therapeutic potential to enhance implantation rates in ARTs. These findings could inform the development of personalized protocols, such as timed administration of embryo-derived factors to optimize endometrial preparedness.

While our study pioneers the use of EEOs to model embryo supernatant–endometrial interactions, several limitations warrant attention. First, the small sample size (n = 4 per group) limits statistical power, necessitating validation in larger cohorts to expand upon the preliminary finding present here. Secondly, a recognized limitation is that we do not know if embryos were aneuploid or euploid, thus, further experiments should use PGT-tested embryos. In our samples, the age of the women whose embryos resulted in live birth was younger. As advanced age is highly associated with embryo aneuploidy (Elmerdahl Frederiksen *et al.*, 2024), it is possible that the EEO can detect this feature and future experiments could test embryos with known PGT-A status to validate this hypothesis. Comparing the endometrial response to conditioned media from euploid versus aneuploid embryos within the same EEO system, we could disentangle the endometrial versus the embryonic contribution to the cross-talk dialogue. Once a transcriptomic signature for pregnancy success is elucidated, building on the results presented here, future experiments could utilize this system to explore the endometrial response to embryo supernatants from the same patient, to enable ET decisions for improved outcomes. We used, for these studies, EEO generated from a patient with proven fertility, and whether EEO derived from patients with reproductive pathologies responds to the embryonic signals in a similar manner remains to be determined.

Conclusion

By demonstrating the embryo's capacity to actively remodel the endometrial transcriptome, this work advances our understanding of implantation biology. The identified pathways, particularly Wnt signaling and cytoskeletal reorganization, offer novel targets for improving ART outcomes. Translating these insights into clinical tools, such as receptivity biomarkers or embryo-conditioned therapies, could address the persistent challenge of implantation failure in infertility treatments.

Supplementary data

Supplementary data are available at *Molecular Human Reproduction* online.

Data availability

Data have been deposited to NCBI BioProject ID: PRJNA1368837; BioSample accessions SAMN53371842, SAMN53371843, SAMN53371844, SAMN53371845, SAMN53371846, SAMN53371847, SAMN53371848, SAMN53371849.

Acknowledgements

We are very grateful to all patients who provided biological samples and data for this study. We would also like to thank all clinical colleagues involved with the collection of samples, in particular Ginny Mounce, Karen Turner, Andrew Thomson, Kate Field, and Jamie Meadows.

Authors' roles

Investigation: Z.J., Y.W., A.F.B., H.R.-C., R.D., T.C., L.W.; Methodology: Z.J., A.F.B., R.D.; Data Curation: Z.J., Y.W., L.W., P. M., I.G.; Project Administration: P.M., T.C.; Resources: T.C.; Conceptualization: J.H.S.; Supervision and Design: P.M., C.M.B., I. G., J.H.S.; Writing of original draft: Z.J., Y.W.; Review and editing: H.R.-C., A.F.B., C.M.B., J.H.S.; Funding Acquisition: I.G., J.H.S. All authors reviewed the final version of the manuscript prior to publication.

Funding

This work was supported by funding by University of Oxford Medical Sciences Internal Fund (Ref. 0014469), the Academy of Medical Sciences, Springboard award (SBF007\100078), and the National Natural Science Foundation of China (No. 82001523).

Conflict of interest

The authors have no conflicts of interest to declare.

References

Aplin JD, Ruane PT. Embryo-epithelium interactions during implantation at a glance. *J Cell Sci* 2017;**130**:15–22.

Ashary N, Tiwari A, Modi D. Embryo implantation: war in times of love. *Endocrinology* 2018;**159**:1188–1198.

Awonuga AO, Camp OG, Abu-Soud HM, Rappolee DA, Puscheck EE, Diamond MP. Determinants of embryo implantation: roles of the endometrium and embryo in implantation success. *Reprod Sci* 2023;**30**:2339–2348.

Boretto M, Cox B, Noben M, Hendriks N, Fassbender A, Roose H, Amant F, Timmerman D, Tomassetti C, Vanhie A *et al.* Development of organoids from mouse and human endometrium showing endometrial epithelium physiology and long-term expandability. *Development* 2017;**144**:1775–1786.

Carson SA, Kallen AN. Diagnosis and management of infertility: a review. *JAMA* 2021;**326**:65–76.

Cho CJ, Park D, Mills JC. ELAPOR1 is a secretory granule maturation-promoting factor that is lost during paligenosis. *Am J Physiol Gastrointest Liver Physiol* 2022;**322**:G49–G65.

Cuman C, Menkhorst EM, Rombauts LJ, Holden S, Webster D, Bilandzic M, Osianlis T, Dimitriadis E. Preimplantation human blastocysts release factors that differentially alter human endometrial epithelial cell adhesion and gene expression relative to IVF success. *Hum Reprod* 2013;**28**:1161–1171.

da Silva FAR, Pascoal LB, Dotti I, Setsuko Ayrizono ML, Aguilar D, Rodrigues BL, Arroyes M, Ferrer-Picon E, Milanski M, Velloso LA *et al.* Whole transcriptional analysis identifies markers of B, T and plasma cell signaling pathways in the mesenteric adipose tissue associated with Crohn's disease. *J Transl Med* 2020;**18**:44.

Das SK, Wang XN, Paria BC, Damm D, Abraham JA, Klagsbrun M, Andrews GK, Dey SK. Heparin-binding EGF-like growth factor gene is induced in the mouse uterus temporally by the blastocyst solely at the site of its apposition: a possible ligand for interaction with blastocyst EGF-receptor in implantation. *Development* 1994;**120**:1071–1083.

Elmerdahl Frederiksen L, Olgaard SM, Roos L, Petersen OB, Rode L, Hartwig T, Ekelund CK; Danish Central Cytogenetics Registry Study Group; Vogel I. Maternal age and the risk of fetal aneuploidy: A nationwide cohort study of more than 500 000 singleton pregnancies in Denmark from 2008 to 2017. *Acta Obstet Gynecol Scand* 2024;**103**:351–359.

Fitzgerald HC, Dhakal P, Behura SK, Schust DJ, Spencer TE. Self-renewing endometrial epithelial organoids of the human uterus. *Proc Natl Acad Sci USA* 2019;**116**:23132–23142.

Gardner DK, Lane M, Stevens J, Schlenker T, Schoolcraft WB. Blastocyst score affects implantation and pregnancy outcome: towards a single blastocyst transfer. *Fertil Steril* 2000;**73**:1155–1158.

Geng M, Xu K, Meng L, Xu J, Jiang C, Guo Y, Ren X, Li X, Peng Y, Wang S *et al.* Up-regulated DERL3 in fibroblast-like synoviocytes exacerbates inflammation of rheumatoid arthritis. *Clin Immunol* 2020;**220**:108579.

Huang A, Qin C, Wu M, Zhang D, Wu G, Sun P. ELAPOR1 suppresses tumor progression in colorectal cancer and indicates favorable prognosis. *Cancer Biomark* 2023;**37**:279–288.

Kim HJ, Lee S, Lee HY, Won H, Chang SH, Nah SS. 15-hydroxyprostaglandin dehydrogenase is upregulated by hydroxychloroquine in rheumatoid arthritis fibroblast-like synoviocytes. *Mol Med Rep* 2015;**12**:4141–4148.

Li X, Kodithuwakku SP, Chan RWS, Yeung WSB, Yao Y, Ng EHY, Chiu PCN, Lee CL. Three-dimensional culture models of human endometrium for studying trophoblast-endometrium interaction during implantation. *Reprod Biol Endocrinol* 2022;**20**:120.

Lin L, Lin G, Lin H, Chen L, Chen X, Lin Q, Xu Y, Zeng Y. Integrated profiling of endoplasmic reticulum stress-related DERL3 in the prognostic and immune features of lung adenocarcinoma. *Front Immunol* 2022;**13**:906420.

Lopez-Serra P, Marcilla M, Villanueva A, Ramos-Fernandez A, Palau A, Leal L, Wahi JE, Setien-Baranda F, Szczesna K, Moutinho C *et al.* A DERL3-associated defect in the degradation of SLC2A1 mediates the Warburg effect. *Nat Commun* 2014;**5**:3608.

Lou L, Kong S, Sun Y, Zhang Z, Wang H. Human endometrial organoids: recent research progress and potential applications. *Front Cell Dev Biol* 2022;**10**:844623.

Mackens S, Santos-Ribeiro S, van de Vijver A, Racca A, Van Landuyt L, Tournaye H, Blockeel C. Frozen embryo transfer: a review on the optimal endometrial preparation and timing. *Hum Reprod* 2017;**32**:2234–2242.

Mareckova M, Garcia-Alonso L, Moullet M, Lorenzi V, Petryszak R, Sancho-Serra C, Oszlanczi A, Icoresi Mazzeo C, Wong FCK, Kelava I *et al.* An integrated single-cell reference atlas of the human endometrium. *Nat Genet* 2024;**56**:1925–1937.

Meng J, Zong C, Wang M, Chen Y, Zhao S. Constructing a prognostic model of uterine corpus endometrial carcinoma and predicting drug-sensitivity responses using programmed cell death-related pathways. *J Cancer* 2024;**15**:2948–2959.

Mishra A, Ashary N, Sharma R, Modi D. Extracellular vesicles in embryo implantation and disorders of the endometrium. *Am J Reprod Immunol* 2021;**85**:e13360.

Oda Y, Okada T, Yoshida H, Kaufman RJ, Nagata K, Mori K. Derlin-2 and Derlin-3 are regulated by the mammalian unfolded protein response and are required for ER-associated degradation. *J Cell Biol* 2006;**172**:383–393.

Ohara Y, Liu H, Craig AJ, Yang S, Moreno P, Dorsey TH, Cawley H, Azizian A, Gaedcke J, Ghadimi M *et al.* ELAPOR1 induces the classical/progenitor subtype and contributes to reduced disease aggressiveness through metabolic reprogramming in pancreatic cancer. *Int J Cancer* 2024;**155**:569–581.

Parks JC, McCallie BR, Patton AL, Al-Safi ZA, Polotsky AJ, Griffin DK, Schoolcraft WB, Katz-Jaffe MG. The impact of infertility diagnosis on embryo-endometrial dialogue. *Reproduction* 2018; **155**:543–552.

Rodriguez M, Kang EY, Farrington K, Cook LS, Le ND, Karnezis AN, Lee CH, Nelson GS, Terzic T, Lee S *et al.* Accurate Distinction of Ovarian Clear Cell From Endometrioid Carcinoma Requires Integration of Phenotype, Immunohistochemical Predictions, and Genotype: Implications for Lynch Syndrome Screening. *Am J Surg Pathol* 2021;**45**:1452–1463.

Siehler J, Bilekova S, Chapouton P, Dema A, Albanese P, Tamara S, Jain C, Sterr M, Enos SJ, Chen C *et al.* Inceptor binds to and directs insulin towards lysosomal degradation in beta cells. *Nat Metab* 2024;**6**:2374–2390.

Sun CC, Zhou ZQ, Yang D, Chen ZL, Zhou YY, Wen W, Feng C, Zheng L, Peng XY, Tang CF. Recent advances in studies of 15-PGDH as a key enzyme for the degradation of prostaglandins. *Int Immunopharmacol* 2021;**101**:108176.

Tepekoy F, Akkoyunlu G, Demir R. The role of Wnt signaling members in the uterus and embryo during pre-implantation and implantation. *J Assist Reprod Genet* 2015;**32**:337–346.

Thoma ME, McLain AC, Louis JF, King RB, Trumble AC, Sundaram R, Buck Louis GM. Prevalence of infertility in the United States as estimated by the current duration approach and a traditional constructed approach. *Fertil Steril* 2013;**99**:1324–1331.e1.

Ye Y, Shibata Y, Yun C, Ron D, Rapoport TA. A membrane protein complex mediates retro-translocation from the ER lumen into the cytosol. *Nature* 2004;**429**:841–847.

Molecular Human Reproduction, 2026, 32, 1–11
https://doi.org/10.1093/molehr/gaaf062
Original Research